Observation of Self Absorption of Mercury I and Cadmium I Emission in an Atmospheric Microwave Sustained Plasma

Kamal Hadidi*, Paul Woskov, Karyn Green, Paul Thomas
Plasma Science and Fusion Center
Massachusetts Institute of Technology
Cambridge, MA 02139

Summary

Atomic emission spectroscopy of a continuous, atmospheric-pressure microwave sustained plasma in an undiluted slip stream of stack exhaust is under development for real-time monitoring of EPA regulated hazardous metals (As, Be, Cd, Cr, Hg, and Pb). The detection limit in such a plasma for two of these metals on their strongest transitions, Cd I 228.8 nm and Hg I 253.65 nm, has been found to depend on the path length between the plasma and the detection system. Measurements were carried out on long plasma columns >100 mm x ~10 mm diameter sustained in air by approximately 1.5 kW power at 2.45 GHz. The detection limit using a long path-length axial view for UV light collection versus short path-length side views at different points along the plasma column have shown a clear diminution of the signal for the axial view. Self-absorption by unexcited atomic cadmium and mercury is shown to be responsible for diminution of the axial signal. The Cd I 228.8 nm transition was observed to reverse from an emission feature to an absorption feature when the axial path-length was increased.

Introduction

Because of public concern and the health problems they can cause, tougher regulations are being proposed for stack emissions of hazardous metals such as mercury, cadmium, and arsenic, which will require real time monitoring. Many industrial plants such as power plants, thermal processing plants and other industrial sources will need such monitors. Until recently, no continuous monitoring method for metals was available. In the USA, the Environmental Protection Agency (EPA) uses Method 29 for testing metals emissions compliance with clean air regulations. However, this method is not real-time, only providing a historical record of emissions. It requires the taking of a sample from the stack and having it analyzed in the laboratory. This process can take days before the results are known. To our knowledge, there is only one commercial real-time metals monitoring system available on the market[1]. Improvements are still needed in measurement accuracy, sensitivity, and affordability of continuous emission monitors (CEMs) for metals.

Several methods that make use of plasmas for atomic emission spectroscopy (AES) of trace metals are being developed as CEMs. Some of these methods such as inductively coupled plasma (ICP)[1, 3] and laser induced breakdown spark (LIBS) systems[4, 5] have

* Corresponding author: hadidi@psfc.mit.edu

limitations in one or more of the requirements for accuracy, sensitivity, and the capability for isokinetic sampling. A microwave plasma-based continuous monitor for real-time atomic emission spectroscopy of trace metals in stack exhaust[6] is being developed at MIT Plasma Science and Fusion Center. It can operate continuously in large volume, fast flowing stack exhaust with an attached metals injection system for span calibration. Excellent minimum detection limits and good accuracy have been achieved in air and undiluted stack exhaust for Pb, Be, and Cr[6,7]. Good detection limits have also been achieved for Cd, Hg, and As in pure nitrogen gas plasmas. However, the detection limit for Hg, Cd, and As has been found to degrade significantly in an air plasma[8]. It is important to understand the mechanisms by which the sensitivity for these metals is degraded in order to be able to further optimize this CEM for its intended application.

Previously we have shown that when oxygen is added to a nitrogen plasma, there is a significant reduction in the atomic emission of metals with high excitation energy levels such as mercury and arsenic[8]. Concurrent with the reduction in the metals UV emission, a slight lowering of the atomic excitation temperature was measured. No UV absorption was observed due to ozone or other molecular species in the plasma. Therefore, the effect of oxygen is to reduce the excitation of the atomic metals species in the plasma. Researchers of mercury arc plasmas have also noted a connection between temperature and emission intensity. The net radiative emission from a mercury arc lamp was observed to decreased by two orders of magnitude when the temperature of the plasma decreased from 6000 K to 4500 K[9]. It was concluded that self-absorption in the outer cooler regions of the plasma was needed to explain this result.

In this paper we present experimental measurements that support this argument for the microwave CEM plasma. Self-absorption of atomic emission is observed on strong metal transitions having their lower electronic level in the ground state. Both Cd I 228.8 nm and Hg I 253.65 nm are shown to have stronger self-absorption in plasmas with oxygen, supporting the previous claim that the addition of oxygen to the plasma reduces the atomic excitation of metals with high energy excitation states. The resulting increase in the population of unexcited atomic species causes an increase in UV absorption, compounding the problem of reduced emission of energetic transitions that terminate on the ground state.

Experimental Setup

The experimental setup, as described previously[8] was adapted for UV emission/absorption measurements as shown in Figure 1. A 1.5 kW, 2.45 GHz magnetron source irradiated a gas flow in a dielectric tube (25.4 mm i.d.) transversing a shorted WR-284 (72 x 34 mm) waveguide. The plasma flame was approximately 10 mm in diameter and extended for more than 100 mm from the center of the waveguide. Four slits 10 mm in length and 2 mm wide were cut into the side of the waveguide and in the after glow channel along the plasma column in order to view the plasma from the side, perpendicular to the plasma axis. A detail of these silts is shown in Figure 2. The slits were covered with quartz plates and sealed with RTV in order to prevent air leaks into the

plasma. The boron nitride tube used in previous experiments[8] was replaced with a quartz tube in order to view the plasma from the side.
The side viewing UV light collection optics consisted of a 5 mm diameter, ~10 mm focal length lens positioned on the quartz plate at the center of a slit. The lens focused the light onto a 0.8 mm core fiber optic cable positioned at the focal point. The side viewing optic system was moved from slit to slit for the measurements that are presented here.

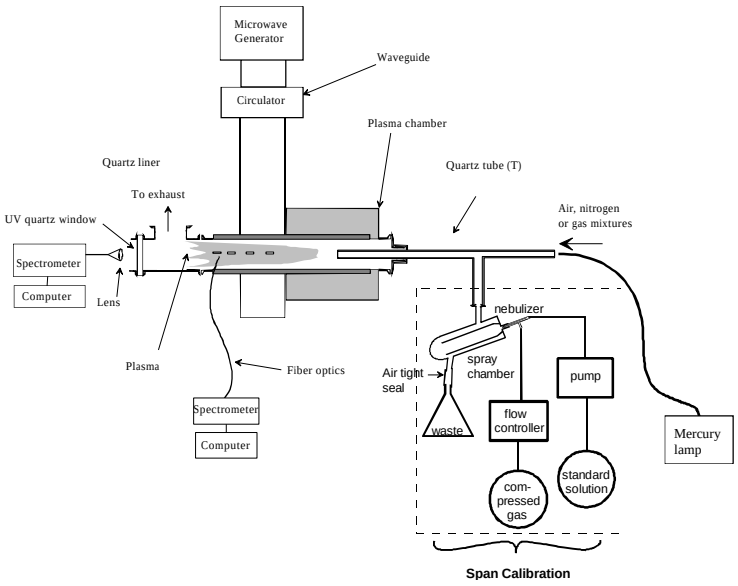

Figure 1. Experimental setup

For most of the experiments, the axial view of the plasma was performed at a distance of 25 cm from the waveguide. The light was collected through a 50 mm diameter quartz window and lens that focused it onto a 0.8 mm core fiber optic cable at a focal length of 75 mm. This optical system was mounted on the axial branch of the plasma exhaust tubing steel Tee (internal i.d. 38 mm) used to connect the exhaust pump to the side. The center of the perpendicular branch of the Tee was 11 cm from the waveguide. For some experiments with cadmium, and to study the effect of a longer path length on emission and absorption, we used a longer Tee. For this Tee, the distance between the waveguide and the optical system was 36 cm, and the distance between the waveguide and the exhaust was 21 cm.

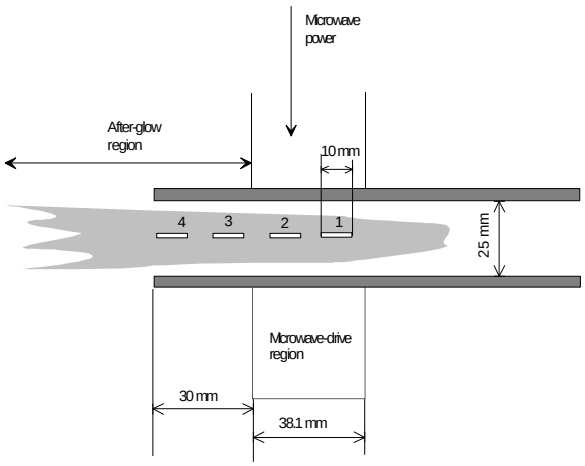

Figure 2. Details of the side measurement setup

The fiber optic cable, which was 2 m long for both side and axial view, was connected to a 0.64 m grating spectrometer with a Princeton Instruments 512-element linear detector array. For each measurement, a set of background spectra was taken first, using clean deionized water, then an aerosol of the desired element was injected and another set of spectra was taken. The aerosol contained either mercury or cadmium at 10,000 µg/ml in a 5% HNO_3 solution. It was assumed that the clean water background was representative of the dilute water/HNO_3 acid background spectrum. The aerosol injection, calibration

system, and the calculation method for the metals concentration in the gas flow were described previously[8].

The base plasma gas flow rates were14 liter per minute of air for the axial sample line flow and 9 l/min nitrogen for the swirl flow, which confined the plasma to the center of the discharge tube. The integration time for data acquisition was 0.1 second and 3 minute data sets of 600 sequential spectra were recorded of each background and metal signal. The first step in the data analysis involved the identification of the relevant detector pixels for a given metal transition and plotting the signal of those pixels as a function of time. The next step consisted of smoothing out the background and the signal over 10 points and then subtracting the background from the metal signal. The results were further averaged for an integration time of 1 min.

The minimum detection limit (MDL) is calculated as 3 times the standard deviation of the signal fluctuations. In units of $\mu g/m^3$ it is given by the following formula:

$$MDL = 3\frac{s}{S}C_{span} \qquad (1)$$

where s is the standard deviation of the signal fluctuations, S is the signal intensity in the same units as the standard deviation, and C_{span} is the concentration of the metal in $\mu g/m^3$ that produces signal S. In our system a pneumatic nebulizer is used to inject a known metals concentration into the plasma and C_{span} is given by:

$$C_{span} = \frac{e\,XR}{F} \qquad (2)$$

Where ε is the nebulizer efficiency for metals transport, X is the standard solution concentration in mg/ml, R is the rate of solution in ml/min pumped into the nebulizer, and F is the volume flow rate of gas in the sample line in m^3/min. The Meinhard Type A pneumatic nebulizer used for this work had a measured metals transport efficiency of 0.9% and the solution uptake rate was nominally 1 ml/min.

Results

Most atomic emission from the microwave plasma is optically thin. Consequently, the longer the path length in the plasma for UV/light collection the higher the emission signal. For this reason the axial optics viewing geometry provides the strongest signals and the lowest detection limits for most metals. In our present setup this includes the strong atomic emission of lead, chromium, and iron. However, in a few important cases the opposite is true. This includes the primary transitions used for monitoring cadmium and mercury.

Figures 3 and 4 show the measured minimum detection limit (MDL) and standard deviation for Cd I 228.8 nm and Hg I 253.65 nm lines, respectively. The plots are a function of the different light collection views, the four side views from the waveguide

out to the afterglow and the axial view. The MDL is lowest for the side views. For Cd I 228.8 nm the MDL is at its minimum at side 2 where it reaches 38 μg/m^3 and increases sharply for axial viewing to 1292 μg/m^3. For the Hg I 253.65 nm the MDL also reaches its minimum at side 2 at 73 μg/m^3 then increases to a maximum at side 4 of 128 μg/m^3. It decreases to 91 μg/m^3 for the axial view, but is still higher than the best side view limit.

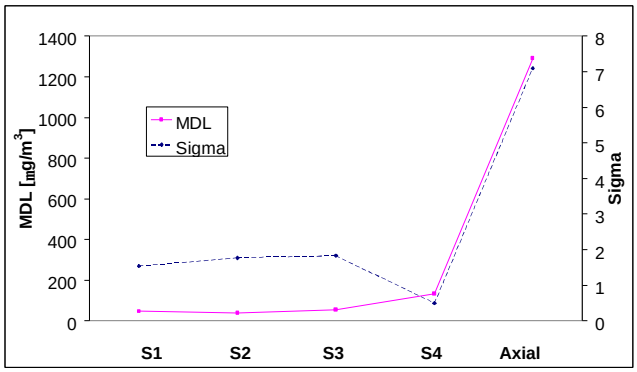

Figure 3. Minimum detection limit (MDL) and standard deviation (sigma) for Cd I 228.8 nm

The standard deviation of the signal fluctuations are also low for the side views for both these transitions and then increase to a maximum for the axial view. This increase in the standard deviation more than offsets stronger axial signals to make the axial view MDL higher as calculated by equation (1). Both these cadmium and mercury transitions terminate on ground states making them susceptible to absorption by unexcited cadmium and mercury atoms. However, the fact that a transition terminates on a ground state is not sufficient by itself to cause a transition to have a higher detection limit for the longer path-length axial view.

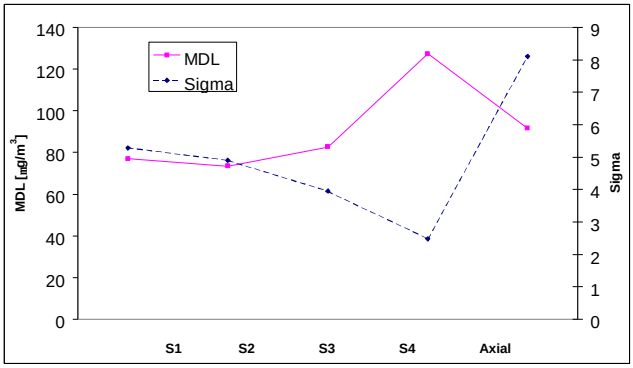

Figure 4. Minimum detection limit (MDL) and standard deviation (sigma) for Hg I 253.65 nm

This is demonstrated by measurements taken on the Cd I 326.1 nm line, also a ground state terminating transition, shown in Figure 5. As can be seen, the MDL for this line decreases from 166 μg/m^3 for side 1, to 68 μg/m^3 for side 2. It increases again for side 3 and side 4 to reach 132 μg/m^3, then it dramatically decreases to reach a minimum at 8 μg/m^3 for the axial view.

The low axial MDL for the Cd I 326.1 nm transition is due primarily to a significant increase in UV signal levels when the collection optics view axially, as is the case for most axial atomic emission. The MDL is a minimum despite a maximum for the axial signal standard deviation. Figure 5 shows that the standard deviation stays approximately constant at a low value from side 1 to side 4 and then increases sharply for the axial view. The increase in axially collected UV emission levels more than compensates for this increase in signal fluctuations to result in a low MDL as calculated by equation (1).

The sharp increase in the standard deviation of the axial viewed signal for all atomic emission suggests that turbulence in the plasma afterglow could be an important mechanism suppressing the MDL. Turbulence is present because the exhaust flow must make a sharp 90° bend 11-cm from the waveguide.

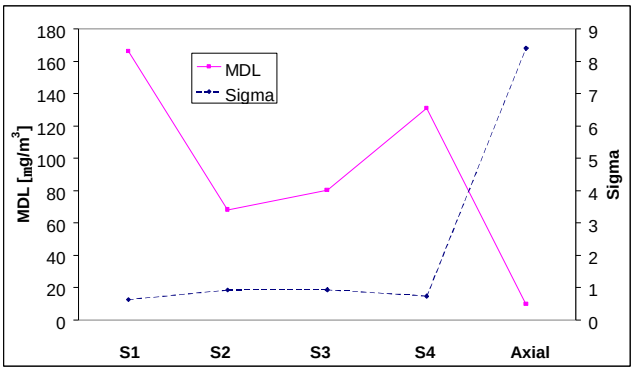

Figure 5. Minimum detection limit (MDL) and standard deviation (sigma) for Cd I 326.1 nm

An extension was added to the exhaust Tee to move this turbulent region further away (21 cm) from the waveguide and plasma UV emission region. The resulting axial spectra for this longer axial path length clearly showed that self-absorption by unexcited atoms is the dominate mechanism for reducing the MDL of Cd I 228.8 nm and Hg I 253.65 nm.

Figure 6 shows spectra of Cd I 228.8 nm and Cd II 226.5 nm. In figure 6a the emission spectrum is for the shorter axial length and shows the two cadmium transitions in emission. In figure 6b the axial length is 11 cm longer and the Cd I 228.8 nm transition reverses into an absorption feature. There is no change in the Cd II 226.5 emission because this line is not absorbed by unexcited atomic cadmium. Similar spectra for Hg I 253.65 nm emission did not produce an absorption feature, but the emission level on this line was significantly reduced for the longer axial path length.

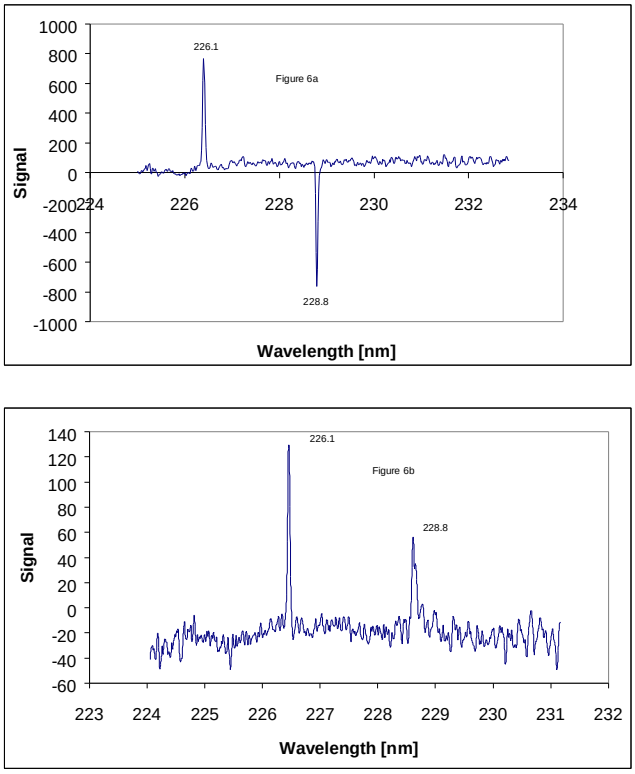

Figure 6b. Spectra of Cd I 228.8 nm and Cd II 226.5 nm a) the emission spectrum is for the shorter axial length and shows the two cadmium transitions in emission. In figure 6b the axial length is 11 cm longer and the Cd I 228.8 nm transition reverses into an absorption feature.

Discussion

The Cd I 228.8 nm emission is a $5p(^1P^o_1) \rightarrow 5s^2(^1S_o)$ transition with an excitation energy of 5.42 eV and the Hg I 253.65 nm emission is a $6p(^3P^o_1) \rightarrow 6s^2(^1S_o)$ transition with an excitation energy of 4.89 eV. The mercury transition is a forbidden transition, violating the selection rule against singlet-triplet transitions. Consequently, this mercury transition has a weaker absorption oscillator strength (0.0245) [10] than the Cd I 228.8 nm transition (1.4). This would explain the higher degree of self-absorption observed on the cadmium line. Also the high excitation energy would explain why the optimum side-viewing region for these transitions is at side 2. It is here that the metals aerosol has had the longest residence time in the plasma to be volatilized while still being in the waveguide. The high microwave electric fields in the waveguide generate the energetic electrons that excite these transitions. The energetic electrons would be quickly collisionaly quenched up stream of the waveguide and therefore excitation of these energetic states would not be as efficient outside the waveguide.

The Cd I 326.1 nm emission is a $5p(^3P^o_1) \rightarrow 5s^2(^1S_o)$ transition with an excitation energy of 3.80 eV. This cadmium transition is the same singlet-triplet transition as the Hg I 253.65 nm transition but at electronic level 5 instead of 6. Therefore, this is also a forbidden transition, but in this case the selection rule against singlet-triplet transitions holds more strongly. The absorption oscillator strength of Cd I 326.1 nm (0.0019) is three orders of magnitude weaker than that for the Cd I 228.8 nm transition and over an order of magnitude weaker than the Hg I 253.65 nm transition. This would account for the lack of observing self-absorption for this longer wavelength cadmium transition.

The observed diminution of the detection limit for mercury and cadmium (on the 228.8 nm transition) in an air plasma is the combination of three effects. First, oxygen in the air reduces the excitation of the energetic metal transitions creating a higher population of unexcited atomic species. The second effect is then absorption by these unexcited atoms that further reduces emission due to the weaker atomic excitation. The third effect is the increased signal fluctuations due to combined fluctuations in both absorption and emission. According to equation (1) the MDL is not only inversely effected by signal strength, but is also proportional to signal noise.

The experimental measurements presented here show that the absorption becomes stronger with increased light collection path length through the plasma, particularly axially through the afterglow region where the population of unexcited atoms would be at a maximum. The extreme case being that shown in figure 6b when the path length is long enough to reverse an atomic emission feature into an atomic absorption feature. Even for short paths through the side of the plasma self-absorption would effect the signals because of a gradient in the temperature distribution due to the swirl flow, which keeps the plasma from attaching to the dielectric walls. However the self-absorption would be kept to a minimum due to the short path length.

Another advantage of the side view is a more stable plasma. The increased self-absorption along the axial view is aggravated by viewing through the most turbulent gas

flow region in the afterglow or beyond where the plasma exhaust makes a sharp turn. Such a diversion of the exhaust flow is necessary to provide axial viewing access. The absorbing species in the turbulent region greatly increases the signal fluctuations from a more stable emission region behind the turbulent region. We briefly examined the possibility of monitoring cadmium using the Cd I 228.8 nm line in absorption and found the detection limit to be much higher than viewing this transition in emission from the side.

Conclusion

The development of a multi-metal CEM for stack emissions using atomic emission spectroscopy requires operation with non-ideal plasma conditions to insure accurate sampling of the stack exhaust. Unlike laboratory ICPs and microwave induced plasmas where a noble gas matrix and flow rate are carefully controlled to achieve maximum sensitivity, a stack mounted CEM must operate with a molecular gas matrix such as air and at high velocity gas flow rates to achieve isokinetic sampling for accuracy. The atmospheric microwave sustained plasma has been shown to be very good at stable operation under such conditions. It can operate continuously in larger volumes and faster flows with lower power than any other stack plasma excitation method demonstrated to date. However, in order to best exploit this capability for application to metals monitoring it is necessary to better understand the details of the plasma atomic emission process under a wider ranged of plasma conditions. This would be true for any *in situ* plasma excitation method.

In the study presented here it has been shown that self-absorption of atomic emission lines occurs in a microwave-sustained air plasma for mercury at 253.65 nm and cadmium at 228.8 nm. Consequently, when picking emission transitions to monitor metals and setting up the UV light collection optics self-absorption must be considered. In the case of cadmium a line other than Cd I 228.8 nm without a strong absorption oscillator strength can be used for monitoring. For mercury, where another strong emission line for monitoring is not available, we need to locate the UV collection optics where the Hg I 253.65 nm excitation is a maximum and minimize the UV light propagation path length through regions having unexcited atomic mercury. This requires locating the UV collection optics as near as possible to the microwave driven region. With appropriate design, atmospheric microwave-sustained plasma should be capable of monitoring all hazardous metals simultaneously for insuring compliance of stack emissions with EPA regulations.

Acknowledgments

The authors acknowledge the support of the Mixed Waste Focus Area, Office of Science and Technology, Environmental Management, U.S. DOE.

References

1 G. A. Meyer, Proceedings of SPIE, Vol. 3534, Environmental Monitoring and Remediation Technologies, Boston, Nov. 1998, 677.

2 C. Trassy, R. Diemiaszonek, P. Pasquini, and R. Meunier: Proc. of Int. Sym. on Environmental Technologies, Plasma System and Applications, Atlanta, 1995, 401.

3 M. D. Seltzer and R. B. Green: Process Control and Quality. 1994, **6** No. 1, 37.

4 D. W. Hahn: Appl. Phys. Lett. 1998, **72**, 2960.

5 J. P. Singh, Fang-Yu Yueh, Hansheng Zhang, R.L. Cook: Process Control and Quanlity 1997, **10**, 247.

6 P. P. Woskov, K. Hadidi, P. Thomas, K. Green, and G. J. Flores, Univ. Calif. Irvine, Proceedings of the IT3 Conference, Session 15, Orlando, USA, May, 1999. www.psfc.mit.edu/library/99ja/99ja011/99ja011_abs.html

7 P.P. Woskov, K. Hadidi, P. Thomas, K. Green, G. Flores, and D. Lamar: Massachusetts Institute of Technology, PSFC/RR-98-1, 1998. www.psfc.mit.edu/library/98rr/98rr001_abs.html

8 K. Hadidi, P.P. Woskov, G.J. Flores, K. Green, P. Thomas: Japaneese Journal of Applied Physics No.7B, Vol.38 (1999) Special issue : Plasma Processing.

9 R.J Zollweg. J. Appl. Phys. 1978, **49**, 3,

10 A. A. Radzig and B. M. Smirnov, Reference Data on Atoms, Molecules and Ions, Chap. 7, Springer-Verlag, Berlin, 1985.